EVALUATION OF A HYBRID CONTROL STRATEGY FOR SHUNT ACTIVE FILTER

João A. Moor Neto[1], Maurício Aredes[1], Edson H.Watanabe[1], Mamour S. Ndiaye[1], Júlio C. Ferreira[1], Samir A. Mussa[2]
[1]COPPE/UFRJ, [2]UNIJUÍ
moor@coe.ufrj.br

Abstract **– In this paper, a control algorithm for sinusoidal current compensation based on Truncated Discrete *Fourier* Transform (TDFT) with variable windowing and a method for *quasi*-instantaneous extraction of the positive-sequence current is proposed for shunt active filters. This hybrid control algorithm of shunt active filter is suitable for three-phase three- and four-wire systems to compensate for harmonic current, current unbalance and reactive power. Simulation and experimental results on a tree-phase three wire scaled down prototype of shunt active filter system using a TMS320F2812 fixed point *DSP* are presented to verify the performance of the proposed control strategy. For a three-phase three-wire system the controller can be implemented based only on seven transducers for voltages and currents measurements.**

Keywords **- Active Filter, Power quality, PLL, Truncated *DFT*, Variable Window.**

I. INTRODUCTION

Power quality problems have been receiving great attention from power system specialists due to their effects for both, utilities and customers. Due to the proliferation of nonlinear loads in distribution systems, specific measures have to be taken to limit current and voltage waveform distortion. Conventionally, LC passive filters have been used to mitigate power quality problems and to compensate for power factor. Nevertheless, in practical situations passive filters have been used as the typical solution for these problems. However, they represent fixed compensation, and may present resonance phenomena with impedances in the system.

The ability of shunt active filter to mitigate current harmonics, current unbalance and reactive power of distribution systems at the utility-customer point of common coupling (PCC) has attracted a great deal of attention [1-2]. Fig. 1 shows the principle of shunt active filter ($i_S = i_C + i_L$).

Different approaches can be used for determining active filter compensation currents, including under operational conditions that voltages at the PCC are unbalanced and even nonsinusoidal.

The shunt active filters controllers can be designed based on time or frequency-domain techniques. Time domain algorithms are based on instantaneous derivation of the compensation currents signals from the distorted and harmonic-polluted current signals. The instantaneous active and imaginary power theory (p-q theory) based controller [2] is an example of time-domain approach.

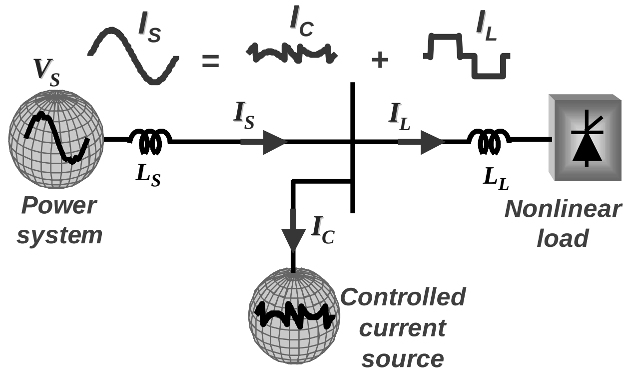

Fig. 1. Principle of shunt current compensation.

Frequency domain algorithms in general are based on *FFT* to extract current disturbance [3]. In this case, it is necessary at least one cycle of the line frequency to extract precisely the disturbance. Another drawback is the number of points in the observation window, which should be a multiple of the number of samples per period. When the value of the fundamental frequency varies around the base frequency (power line frequency) value, this results in a modification in the number of samples per period (window) if constant sampling period is used. Even if there is a slight frequency drift, at that condition, FFT cannot extract precisely the magnitude of the base frequency because FFT is sensitive to frequency variations.

A hybrid control algorithm to control shunt active filter is proposed in this work. This control strategy is based on DFT and a positive-sequence current detector to extract the positive-sequence current component is proposed.

To overcome the speed limitation of DFT algorithm, this algorithm was simplified for calculating only the current or voltage at the fundamental frequency only. Therefore, the simplified algorithm truncates the harmonic calculation and so, hereafter, it is referred to as truncated DFT. The application of this truncated DFT can be improved by a variable windowing, which enable the determination of the waveform fundamental component with more accuracy.

The positive-sequence component of the current is extracted in the time domain by using the main idea shown in [4].

This control technique is flexible and effective for three-phase four-wire and three-phase three-wire active filters under non-sinusoidal and unbalanced voltage source. The validity of this control technique is verified through simulation results using MATLAB and experimental results. The experimental results were obtained by implementing this control algorithm in a Texas Instruments eZdsp™ F2812 fixed point digital signal processor.

II. TRUNCATED DFT WITH VARIABLE WINDOWING

The truncated DFT algorithm was improved by a variable windowing. This algorithm avoids problems related to slight fundamental frequency drift. The window size (number of samples per period) is continuously calculated to track the fundamental frequency of the system voltages by means of a PLL circuit (Phase-locked-loop).

Fig. 2 shows the block diagram for the determination of the number of samples in the observation window of the truncated *DFT* and the fundamental frequency ω_1 calculation.

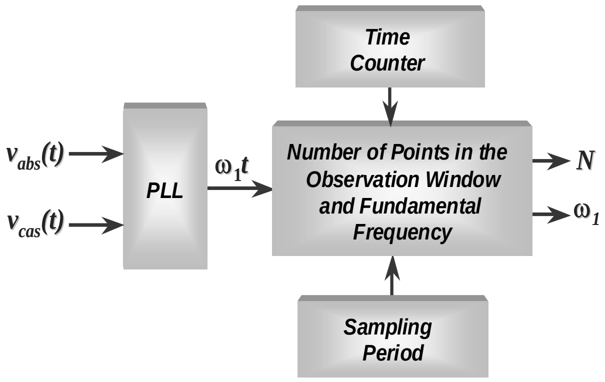

Fig. 2. Block diagram for the determination of the fundamental frequency and number of samples per period.

The fundamental frequency ω_1 and the angular position $\omega_1 t$ obtained by the PLL circuit [5] are necessary to calculate the window size and then define the sampling number of fundamental frequency. Fig. 3 shows the PLL circuit functional block diagram.

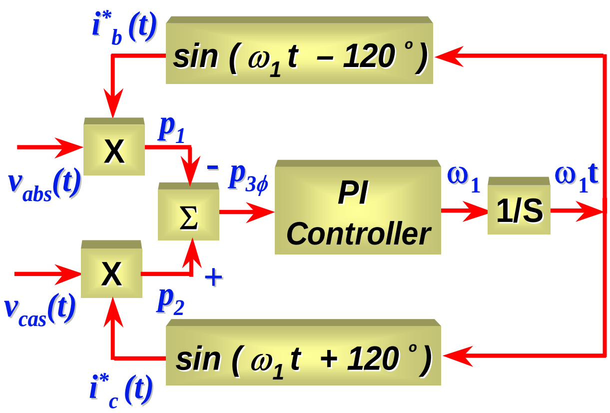

Fig. 3. Functional block diagram of the PLL system.

The angle $\omega_1 t$ varies from $-\pi$ to π with the same period as the fundamental frequency of the system. The zero crossing of this ramp $\omega_1 t$ indicates the beginning of the positive semi-cycle of the sinusoid related to phase a voltage or current. This way, an auxiliary counter is used to count the number n of samples in a semi-cycle starting from the zero crossing of the ramp $\omega_1 t$. The number n is basically equal to half of the number of samples N in a full cycle because this auxiliary counter just counts from 0 to π. To detect the zero crossing of the ramp $\omega_1 t$ it is enough to multiply the actual value of $\omega_1 t$ by its previous value. A positive result indicates that the values of the actual and previous $\omega_1 t$ are above or below zero. A negative result indicates that one of the $\omega_1 t$ samples is above zero and the other is below zero. When the zero crossing of $\omega_1 t$ is verified, the auxiliary counter is reset to zero and it begins to count at each sampling period. When the counter reaches a number n of samples, the frequency of the system is calculated.

Based on the $\omega_1 t$ values and the values of "n", besides the sampling frequency f_s, the actual fundamental frequency ω_1 in which the system is operating is determined by

$$\omega_1 = \frac{\omega_1 t \cdot f_S}{n}. \tag{1}$$

The total number of samples per cycle N that is used in the calculation of the DFT is given as function of the fundamental frequency of operation of the system and the sampling frequency. Considering that the sampling frequency f_s is fixed, the number of samples should vary as the fundamental frequency varies. Therefore, the total number of samples N, corresponding to the actual frequency of operation of the system is given by

$$N = \frac{f_S \cdot 2\pi}{\omega_1}. \tag{2}$$

In this case, was specified a resolution of 0.1 Hz. This way, for a resolution of 0.1 Hz, 600 samples per cycle are necessary. In this way, the sampling frequency was fixed at f_s = 36 kHz.

Assuming that N is the number of samples of a period of the fundamental component of current or voltage signal, the fundamental component can be calculated by the expression of truncated DFT for the fundamental component as

$$\begin{cases} \operatorname{Re} S[1] = \sum_{n=0}^{N-1} s[n]\cos(2\pi n/N) \\ \operatorname{Im} S[1] = \sum_{n=0}^{N-1} s[n]\,sen(2\pi n/N) \end{cases}, \tag{3}$$

where: ReS[1] and ImS[1] correspond to the real and imaginary components of generic signal S at a fundamental frequency of the truncated DFT analysis system.

In this algorithm a counter "J" is used beginning in zero and is increased at each sampling period up to the total number of samples N that is given in (2). Based on this counter "J", an auxiliary ramp of angle "wt_aux" is generated, which serve as input for the sine and cosine functions that is used in the DFT algorithm, as given by,

$$wt\_aux = \left(\frac{2 * N}{N°de\ amostras}\right) * \pi. \tag{4}$$

In each sampling period, the real and imaginary parts of each one of the signals of voltages V and currents I phasors are calculated and accumulated. The real part of the voltage V and current I signals are obtained by the multiplication and accumulation of the signals V and I by cos(wt_aux). In the same way, the imaginary part of the voltage V and current I signals are obtained by the multiplication and accumulation of these signals by sin(wt_aux). These real and imaginary parts are obtained by

$$\begin{cases} V_{real} = V_{real} + V \cdot \cos(wt\_aux) \\ I_{real} = I_{real} + I \cdot \cos(wt\_aux) \\ V_{imag.} = V_{imag.} + V \cdot sin(wt\_aux) \\ I_{imag.} = I_{imag.} + I \cdot sin(wt\_aux) \end{cases} \quad (5)$$

This process begins with J = 0 and it is kept until J = N. In other words, this calculation is made during a complete period of the fundamental frequency of the power system. When J reaches N, the magnitude and phase calculations are started. The information of magnitude and phase, relative to the voltages and currents at each phase are obtained by,

$$\begin{cases} |V_1| = \sqrt{(V_{real}^2 + V_{imag.}^2)} \\ |I_1| = \sqrt{(I_{real}^2 + I_{imag.}^2)} \\ \phi_{V1} = V_{imag.} / V_{real} \\ \phi_{I1} = I_{imag.} / I_{real} \end{cases} \quad (6)$$

After determining the magnitudes and phases of the voltages and currents fundamental components, all V_{real}, $V_{imag.}$, I_{real}, and $I_{imag.}$ parts of the respective signals of voltages and currents are made equal to zero, as well as the counter J. In the next sampling period the process restarts.

III. PRINCIPLE OF THE HYBRID CONTROL STRATEGY

The main idea of the hybrid control algorithm proposed here is to obtain the fundamental positive-sequence component of the load current. These components are appropriate to generate sinusoidal waveforms that are used to extract the disturbance in the currents and generate currents reference signals to drive the shunt active filters to guarantee sinusoidal and balanced compensated current drawn from the source.

Fig. 4 shows the control block diagram of the shunt active filter that realizes the sinusoidal current hybrid control algorithm for three-phase systems.

In this case, the measurements points were reduced to seven, whereas traditional controller usually utilizes ten transducers for voltages and currents measurements. The measurements points adopted were the following:

- line voltages: v_{ab} and v_{ca};
- line currents: i_b and i_c;
- converter currents: i_{bf} and i_{cf};
- DC link voltage: v_{dc}.

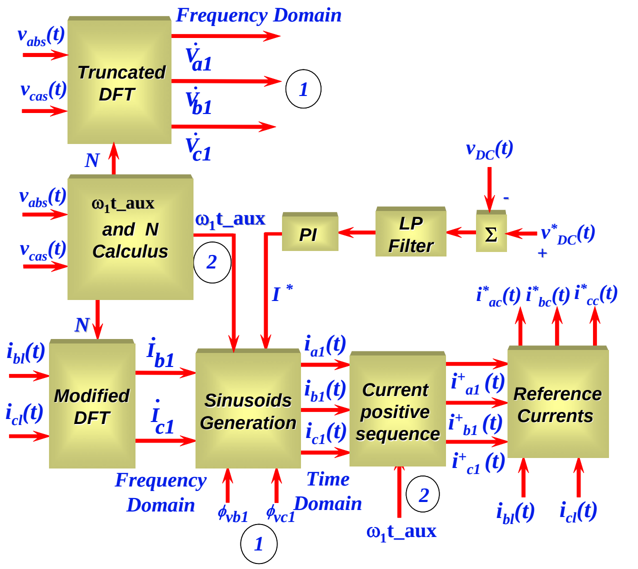

Fig. 4. Block diagram of hybrid control

The calculated positive sequence voltage and currents are given by:

$$\begin{cases} v(t) = \sqrt{2}\,|V_1| \cdot \sin(wt\_aux + \phi_{V1}) \\ i(t) = \sqrt{2}\,|I_1| \cdot \sin(wt\_aux + \phi_{I1}) \end{cases} \quad (7)$$

In this algorithm the real and imaginary parts of the voltage and currents are calculated at each sampling period, not being necessary to store the sampled values.

Haque et al have shown in [4] a *quasi*-positive sequence detector that was adapted here removing the low pass filter of the original circuit configuration. The adapted *quasi*-instantaneous positive sequence detector method is shown in Fig. 5.

The two line voltage phasors $\dot{V}_{ab1} = |V_{ab1}| \angle \phi_{vab1}$ and $\dot{V}_{ca1} = |V_{ca1}| \angle \phi_{vca1}$ are obtained by the application of truncated DFT with variable windowing in the line voltages $v_{ab}(t)$, $v_{ca}(t)$. The phasors of the fundamental component of phase voltages $V_{a1} = |V_{a1}| \angle \phi_{va1}$, $\dot{V}_{b1} = |V_{bs1}| \angle \phi_{vb1}$ and $\dot{V}_{c1} = |V_{c1}| \angle \phi_{vc1}$, can be obtained directly by the phasorial relationship involving sinusoidal waveforms in the classic theory using fundamental component of line voltage phasors $\dot{V}_{ab1}$ and $\dot{V}_{ca1}$.

The phasors of the line currents in the fundamental frequency, $\dot{I}_{b1} = |I_{b1}| \angle \phi_{ib1}$ and $\dot{I}_{c1} = |I_{c1}| \angle \phi_{ic1}$, are calculated applying truncated DFT with variable window in the line currents i_{bl} and i_{cl}.

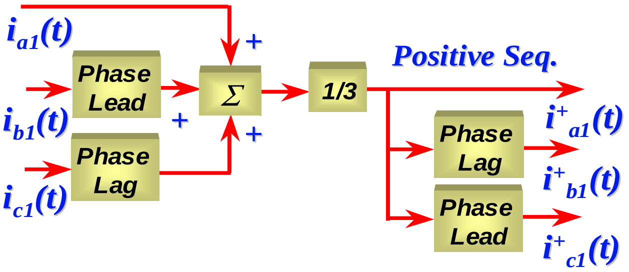

Fig .5. Adapted positive sequence current detector

Considering the magnitudes of the line currents phasors $|I_{b1}|$, $|I_{c1}|$, and the differences between the angles of phases of the voltage phasors ϕ_{vb1}, ϕ_{vc1}, and currents phases ϕ_{ib1}, ϕ_{ic1}, the active part of the actual currents phasors magnitudes is calculated by using the following expression:

$$\begin{cases} |I_{b1W}| = \sqrt{2}\,|I_{b1}|\cos(\phi_{vbs1}-\phi_{ib1}) = \sqrt{2}\,|I_{b1}|\cos(\theta_c) \\ |I_{c1W}| = \sqrt{2}\,|I_{c1}|\cos(\phi_{vcs1}-\phi_{ic1}) = \sqrt{2}\,|I_{b1}|\cos(\theta_c) \end{cases} \quad (8)$$

The magnitudes $|I_{b1W}|$, $|I_{c1W}|$ are used together with the auxiliary signal of control I*, besides the angles of phases of the voltage ϕ_{vb1}, ϕ_{vc1}, to form two new current phasors: $\dot{I}_{b1\_new} = \left(|I_{b1}| + I^*\right)\angle\phi_{vbs1}$ and $\dot{I}_{c1\_new} = \left(|I_{c1}| + I^*\right)\angle\phi_{vcs1}$. The magnitudes of these new currents phasors are used to generate two sinusoidal signals in the fundamental frequency, as given by

$$\begin{cases} i_{b1}(t) = \left(|I_{b1W}| + I^*\right) sen\left(\omega_1 t + \phi_{bv1}\right) \\ i_{c1}(t) = \left(|I_{c1W}| + I^*\right) sen\left(\omega_1 t + \phi_{cv1}\right) \end{cases} \quad (9)$$

The phase *a* current in the fundamental frequency i_{a1} is determined by

$$i_{a1}(t) = -i_{b1}(t) - i_{c1}(t). \quad (10)$$

The auxiliary control signal I^* regulates the exchange of energy between the converter and the AC source in such a way that the losses in the active filter are compensated and the DC link voltage is kept regulated.

These three sinusoidal currents i_{a1}, i_{b1}, i_{c1} are applied to the positive sequence detector shown in Fig. 4. In this way, the fundamental positive-sequence component of line currents $i^+_{a\_1}$, $i^+_{b\_1}$, $i^+_{c\_1}$ are obtained.

The phase *a* load current i_{al} is calculated using the two others line currents

$$i_{al}(t) = -i_{bl}(t) - i_{cl}(t). \quad (11)$$

The reference currents i^*_{ac}, i^*_{bc}, i^*_{cc}, are calculated by

$$\begin{cases} i^*_{ac}(t) = i^+_{a\_1}(t) - i_{al}(t) \\ i^*_{bc}(t) = i^+_{b\_1}(t) - i_{bl}(t) \\ i^*_{cc}(t) = i^+_{c\_1}(t) - i_{cl}(t) \end{cases} \quad (12)$$

These reference currents i^*_{ac}, i^*_{bc}, i^*_{cc} are the input to the PWM current control. Fig. 6 shows the block diagram de PWM current control adopted [6]. The currents i_{af}, i_{bf}, i_{cf} are inverter ac side currents.

This control guarantees a constant switching frequency fixed. The positive sequence phase voltages v^+_{a1}, v^+_{b1}, v^+_{c1} used in this control are calculated in two steps.

- First step, the phasors of the fundamental component of phase voltages $\dot{V}_{a1} = |V_{a1}|\angle\phi_{va1}$, $\dot{V}_{b1} = |V_{b1}|\angle\phi_{vb1}$ and $\dot{V}_{c1} = |V_{c1}|\angle\phi_{vc1}$ are calculated by using DFT;

- Second step, based on the voltage phasors $\dot{V}_{a1}$, $\dot{V}_{b1}$, $\dot{V}_{c1}$, three sinusoids are generated by using the expression (13).

$$\begin{cases} v_{a1}(t) = \sqrt{2}\,|V_{a1}|\sin(\omega_1 t + \phi_{av1}) \\ v_{b1}(t) = \sqrt{2}\,|V_{b1}|\sin(\omega_1 t + \phi_{bv1}) \\ v_{c1}(t) = \sqrt{2}\,|V_{c1}|\sin(\omega_1 t + \phi_{cv1}) \end{cases} \quad (13)$$

These three sinusoidal voltages v_{a1}, v_{b1}, v_{c1}, are applied to the positive sequence detector shown in Fig. 4. This way, the fundamental positive-sequence components phase voltages obtained the fundamental positive-sequence component of phase voltages v^+_{a1}, v^+_{b1}, v^+_{c1} are obtained.

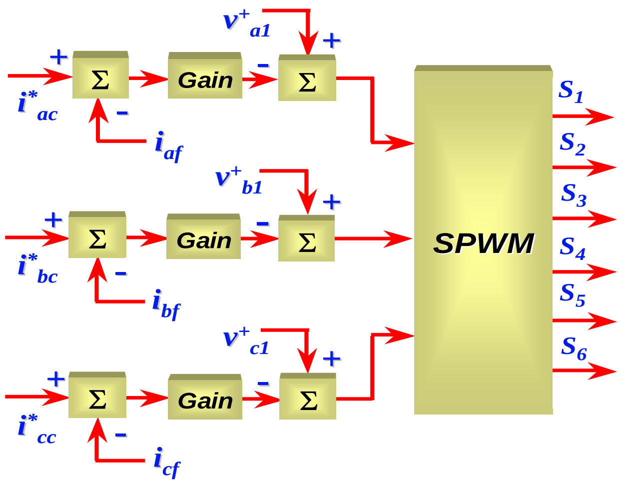

Fig 6. Current PWM Control

IV. SIMULATION AND EXPERIMENTAL RESULTS

A 4.2 kVA laboratory prototype of a shunt active filter was built to verify the hybrid algorithm performance.

Fig. 7 shows the typical system configuration of a three-phase three-wire shunt active filter.

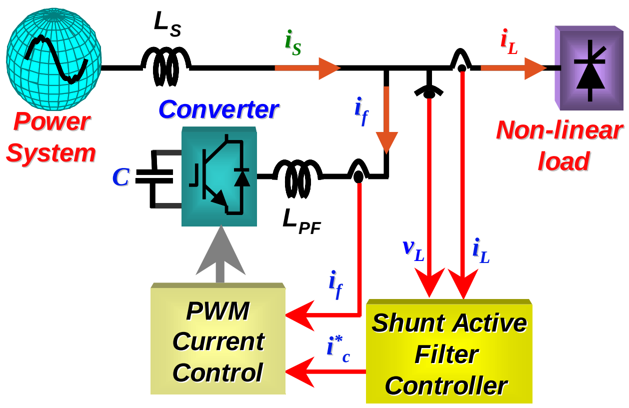

Fig 7. General scheme of the shunt active filter.

Fig. 8 illustrates the three-phase three-wire power circuit diagram of shunt active filter prototype.

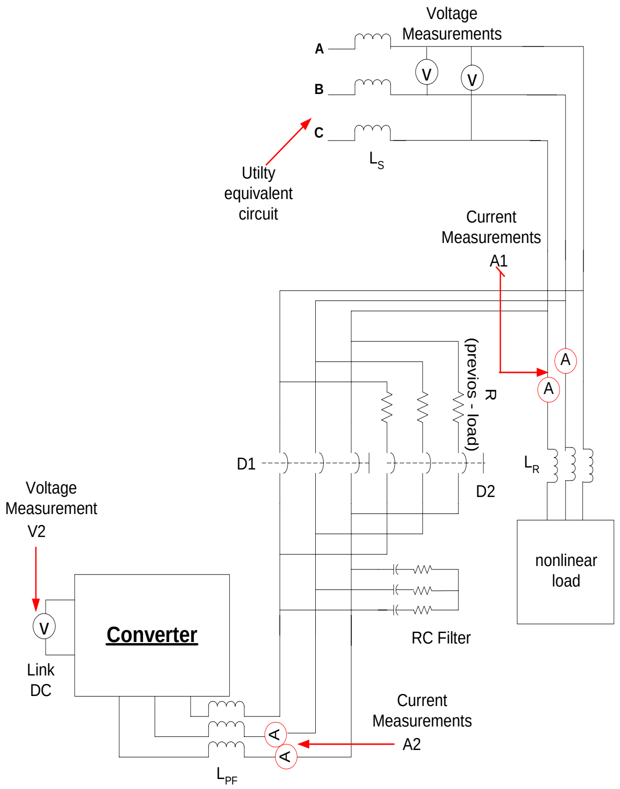

Fig 8. Power circuit diagram of the implemented shunt active filter

In order to implement the three-phase three-wire shunt active filter prototype, a 16 bit fixed-point DSP of TMS320F2812 was used. This laboratory prototype uses IGBT´s as switching elements and the switching frequency was fixed to 10 kHz.

The parameters of the system are:

- Power system inductance: L_S = 0.5 mH;
- Voltage system: V_S = 220 V (line to line);
- Line frequency: f_S = 60 Hz;
- Nonlinear load: three-phase diode rectifier with a resistance R_{DC} = 23 Ω and smoothing inductance L_{DC} = 10 mH.
- Rectifier commutation inductance of L_R = 1.2 mH;
- Inverter commutation inductance: L_{PF} = 1.8 mH;
- RC passive filter: R = 3.2 Ω and C = 20 µF;
- DC link reference voltage: V^*_{DC} = 350 V;

First, MATLAB software package was used for the simulation of the performance of this hybrid control.

Two kinds of simulations are carried out. One is the simulation of the control strategy in C language, and the other is the power circuit of the shunt active filter with Simulink in MATLAB. Due the lack of space, only some simulation results are presented when RC passive filter is connected.

The sampling frequency f_S specified in simulation was 20 kHz.

Fig. 9 shows the source currents after the connection of the active filter. Fig. 10 shows line voltage v_{ab} and source current i_a. Fig. 11 shows phase voltages.

Fig. 12 shows the a-phase source current and a-phase inverter current.

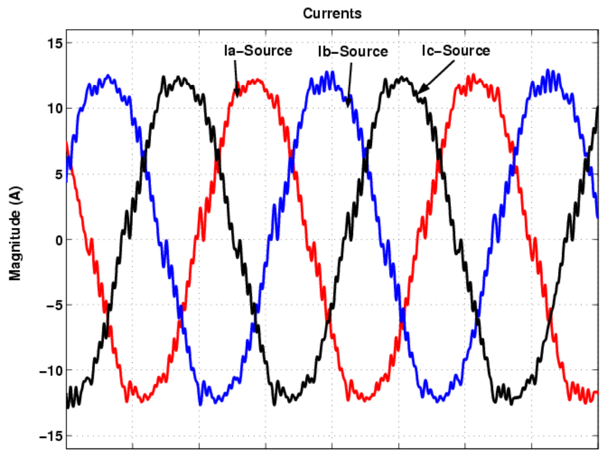

Fig 9. Source currents.

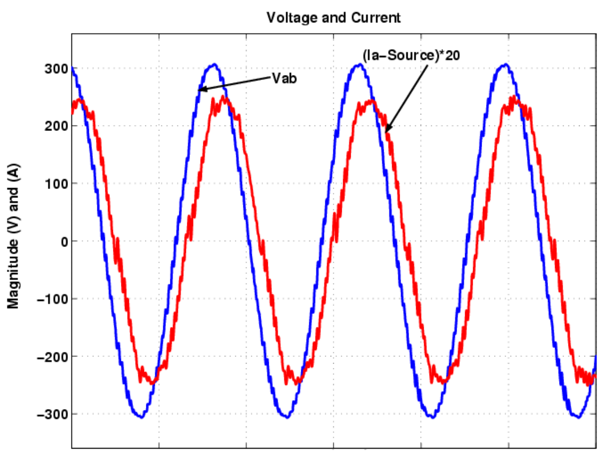

Fig 10. ab-line voltage and a-phase current.

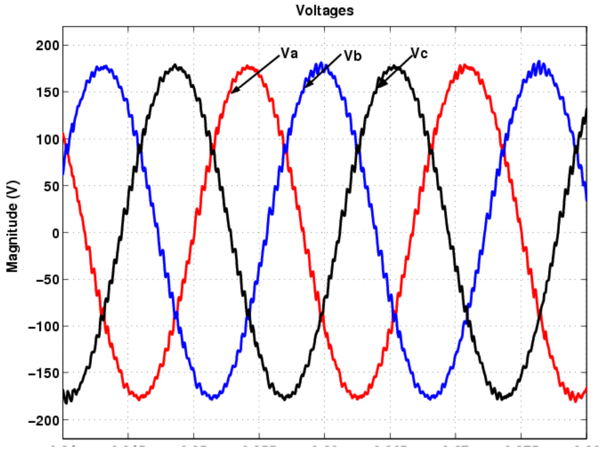

Fig 11. Phase voltages

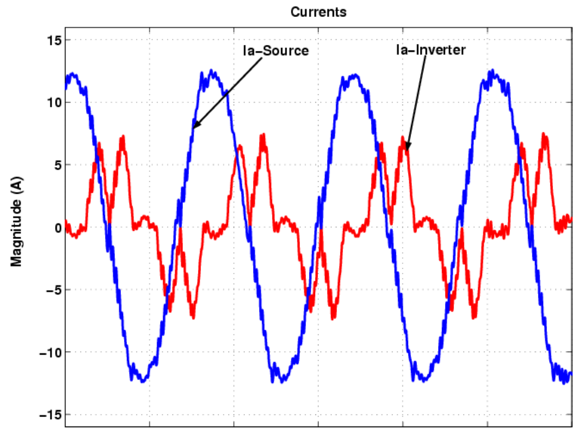

Fig 12. a-phase source and inverter currents

The experimental results are shown in Fig. 13, and Fig. 14. Fig. 13 shows ab-line voltage and a-phase current when active filter is turned-off.

Fig. 14 shows ab-line voltage and a-phase current when active filter is turned-on and passive RC filter is connected.

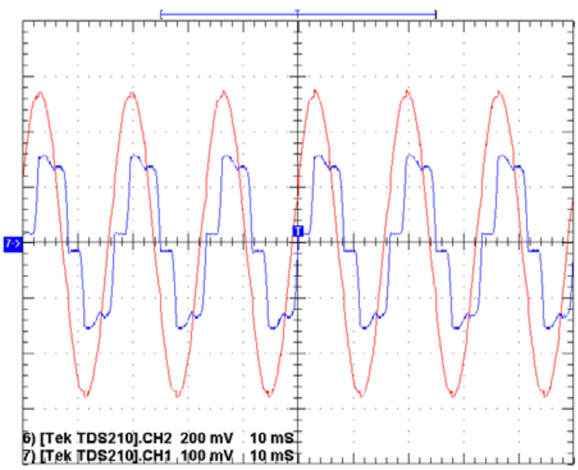

Fig 13. Line voltage V_{ab} and a-phase source current

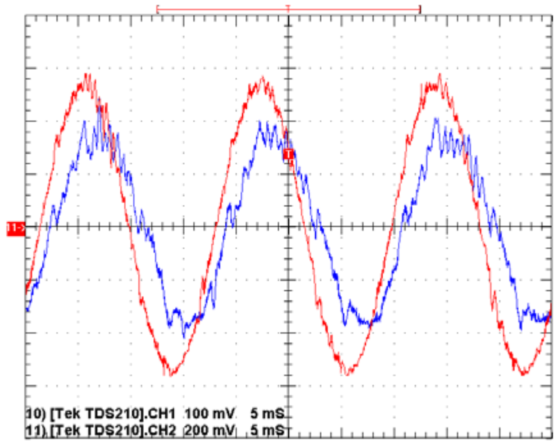

Fig 14. ab-Line voltage and a-phase source current

V. CONCLUSION

A hybrid control algorithm based on a truncated DFT with variable windowing and using the quasi-instantaneous positive sequence of currents shown in [4] has been presented. The truncated DFT requires a short computation time and can be adopted without any problem. The control block utilized to determine the precise quantity of points of the fundamental component shows an improved performance of the truncated DFT. This control block uses a PLL based on instantaneous power theory concepts.

The hybrid control strategy generates reference compensation current references for Shunt Active Filter to compensation for load side current harmonics, current unbalance and reactive power.

REFERENCES

[1] W. M. Grady, M. J. Samotyj and A. H. Noyola, "Survey of Active Power Line Conditioning Methodologies", *IEEE Trans. on Power Delivery*, Vol. 5, No. 3, July 1990, pp. 1536-1542.

[2] H. Akagi and H. Fujita, "A New Line Conditioner for Harmonic Compensation in Power Systems", *IEEE Trans. On Power Delivery*, Vol 10, No. 3, July 1995, pp. 1570-1575.

[3] K. J. P. Macken, et all., "Evaluation of Control Algorithms for Shunt Active Filters Under Unbalanced and Nonsinusoidal Conditions", *in Proc. of 2001 IEEE Porto Power Tech Conference*, Porto, Portugal.

[4] M. T. Haque, S. H. Hosseini and T. Ise, "A Control Strategy for Parallel Active Filters Using Extended p-q Theory and Quasi Instantaneous Positive Sequence Extraction Method", *in Proc. ISIE 2001 – International Symposium on Industrial Electronics*, Pusan 2001, Vol.1, pp. 348-353

[5] M. Aredes, "Active Power Line Conditioners", *Doktor-Ingenieur (Dr.-Ing.) Thesis*, Technisiche Universität Berlin, 1995

[6] F. Z. Peng , J. W. McKeever, D. Adams, "A Power Line Conditioner Using Cascade Multilevel Inverters for Distribution Systems", IEEE Transactions on Industry Applications, Vol. 34, No. 6, November/December 1998